IEEE Access
Multidisciplinary : Rapid Review : Open Access Journal

Received 22 May 2023, accepted 29 May 2023, date of publication 21 June 2023, date of current version 23 June 2023.

Digital Object Identifier 10.1109/ACCESS.2023.3284690

RESEARCH ARTICLE

Investigation of Power Levels Related to Different EMF Exposure Metrics at 6 GHz

WALID EL HAJJ[1], (Member, IEEE), JOHN ROMAN[2], (Senior Member, IEEE), ZHEN YAO[2], (Member, IEEE), ROBERT PAXMAN[2], (Member, IEEE), AND VALERIO DE SANTIS[3], (Senior Member, IEEE)

[1]Intel Corporation, 06600 Antibes, France
[2]Intel Corporation, Hillsboro, OR 97124, USA
[3]Department of Industrial and Information Engineering and Economics, University of L'Aquila, 67100 L'Aquila, Italy

Corresponding author: Valerio De Santis (valerio.desantis@univaq.it)

ABSTRACT New wireless technologies significantly utilize the spectrum around 6 GHz with some of them, like Wi-Fi®6E, using both the spectrum below and above 6 GHz. At these frequencies, the main challenge for electromagnetic field (EMF) exposure assessments is due to the exposure metric changing from specific absorption rate (SAR) to absorbed power density (APD). Moreover, due to current measurement limitations, the incident power density (IPD) rather than APD is used in practice. In this context, the maximum allowed output power to ensure exposure compliance is dependent on the metric used and can lead to a discontinuity below and above 6 GHz even for different channels of the same technology. This paper studies such a discontinuity at the transition frequency of 6 GHz using a dipole antenna and a Planar Inverted F Antenna (PIFA). The study was performed at several exposure distances by means of numerical simulations as well as experimental measurements. The assessment was based on the comparison between maximum power values obtained while remaining compliant to the SAR and IPD limits for the same exposure conditions. The results have shown that for a specific source there was a distance (between 5 and 10 mm) where the highest power reduction for compliance switched from SAR to IPD. The difference or discontinuity level varied between 2 and 6 dB depending on the exposure distance and the source. In summary, SAR is more restrictive at closer distances, while the IPD induces a higher back-off power with an increase in distance.

INDEX TERMS 5G, compliance assessment, EMF exposure, incident power density, specific absorption rate, standardization, Wi-Fi®.

I. INTRODUCTION

New wireless technologies such as 5G and Wi-Fi®6E utilize more and more radio-frequency (RF) spectrum around 6 GHz [1], [2], [3]. At these frequencies, the established adverse effect on biological tissues is of thermal nature and therefore the maximum allowed output power of these devices must be limited to avoid localized heating. Compliance assessment against international safety standards/guidelines [4], [5] is hence an essential procedure to protect from excessive RF electromagnetic field (EMF) exposures.

Around 6 GHz, one of the main challenges for RF-EMF exposure assessments is due to the dosimetric exposure metric changing *de facto*[1] from the specific absorption rate (SAR), i.e., an internal quantity, to the incident power density (IPD), i.e., an external quantity [4], [5]. This yielded in practice to a discontinuity in the maximum allowable output power below and above 6 GHz even for different channels used by the same technology, with inherent issues in determining compliance with international safety standards/guidelines [4], [5].

The first group assessing this issue was an Australian team supported by the Mobile & Wireless Forum (MWF) with

The associate editor coordinating the review of this manuscript and approving it for publication was Stefan Schwarz.

[1]Despite the SAR is an internal quantity, while the IPD is an external quantity, the assessment is related to practical aspects since above 6 GHz the compliance limit of a device is generally defined using IPD metric, while below 6 GHz the compliance limit is defined using SAR.

their companion works related to determine the appropriate RF exposure metric in the frequency range 1-10 GHz using simple planar [6] and complex [7] human body models, respectively. From their studies, it was highlighted as a likely explanation for this discontinuity could be given to the fact that the IPD values have not been formulated for localized exposures but rather for whole-body heating effects.

A few years later, the Ericsson group led by Colombi et al. [8] also pointed out as the large discontinuity in terms of maximum possible radiated power could have negatively affected the deployment of 5G technology when assessing compliance with the exposure limits available at that time.

In 2019 [4] and 2020 [5], the exposure limits at frequencies above 6 GHz have been revised and hence many studies focused on the implications of such revisions above 6 GHz [9], [10], [11], [12], [13], [14], [15], [16], [17], [18], [19], [20]. However, none of these studies investigated the power level discontinuity at the transition frequency of 6 GHz using the revised exposure limits. This paper is therefore the first one addressing the latest power level discontinuity at the transition frequency of 6 GHz using both a dipole antenna and a Planar Inverted F Antenna (PIFA), which can be typically used for Wi-Fi®modular certification as well as host systems.

II. COMPLIANCE ASSESSMENT

In this section, the exposure limits around 6 GHz are firstly presented and the definition of different dosimetric metrics are then provided.

A. EMF EXPOSURE LIMITS AROUND 6 GHz

International safety standards/guidelines have been recently revised by the International Commission on Non-Ionizing Radiation Protection (ICNIRP) [4] and the Technical Committee (TC) 95 of the International Commission on Electromagnetic Safety (ICES) of the Institute of Electrical and Electronics Engineers (IEEE) [5]. The primary changes in these revisions were a change in transition frequency between SAR and PD to 6 GHz, and the introduction of a new exposure metric at frequencies greater than 6 GHz, where the absorbed power density (APD) was defined as the basic restriction (BR) for ICNIRP and the epithelial power density (EPD) as dosimetric reference limit (DRL) for IEEE, respectively. The equivalent incident power density (IPD) in free space is conservatively defined as the reference level (RL) for ICNIRP or exposure reference level (ERL) for IEEE. In the US, the limits provided by the Federal Communication Commission (FCC) also specify SAR below 6 GHz and IPD above [21], but with different exposure limits (see Table 1). It should be noted that no Absorbed/Epithelial PD is specified by FCC.

Even though the ICNIRP specifies that above 6 GHz RLs should not be used to determine compliance, RL and ERL are more practical to conduct compliance assessments compared to the BR or DRL. This is the reason why IPD is taken as a reference dosimetric quantity by some product compliance safety standards established by the

TABLE 1. Exposure limits provided by ICNIRP, IEEE, and FCC for localized exposures in the general public around 6 GHz.[a]

	Frequency (GHz)	Exposure Limit	Spatial Avg.
ICNIRP 2020	≤ 6	SAR[b]: 2 W/kg	10 g
	6 – 30	APD: 20 W/m^2 IPD[c,d]: $55/f_G^{0.177}$	4 cm^2
IEEE C95.1™-2019	≤ 6	SAR[b]: 2 W/kg	10 g
	6 – 30	EPD: 20 W/m^2 IPD[c]: $55/f_G^{0.177}$	4 cm^2
FCC	≤ 6	SAR[b]: 1.6 W/kg	1 g
	6 – 100	IPD: 10 W/m^2	4 cm^2

[a] SAR and PD limits are to be averaged over 6 min.
[b] head and torso.
[c] f_G is frequency in GHz.
[d] within the reactive near-field zone RLs cannot be used to determine compliance, so BRs must be assessed.

International Electro-technical Commission (IEC)-TC106 and IEEE-ICES-TC34. These dual-logo working groups recently released two technical standards aimed to assess exposure to IPD from 6 GHz to 300 GHz both experimentally [22] and numerically [23]. From 6 to 10 GHz an IEC Publicly Available Specification (PAS) has also been published to provide a method to convert SAR to APD for the assessment of human exposure to RF EMFs from wireless devices in close proximity to the head and body [24].

B. DOSIMETRIC ASSESSMENT

Below 6 GHz, the SAR must be assessed. It is defined as:

$$\mathrm{SAR}\left(\mathbf{r}\right)=\frac{\sigma\left(\mathbf{r}\right)}{2\rho\left(\mathbf{r}\right)}\left\|\mathbf{E}\left(\mathbf{r}\right)\right\|^{2} \tag{1}$$

where σ represents the tissue conductivity (S/m), ρ is the mass density (kg/m^3), r denotes the position vector (m), and$\mathbf{E}$ denotes the complex electric field inside the body (V/m). The SAR must be averaged over a tissue cubic mass of 1 g (FCC) or 10 g (ICNIRP and IEEE). Among these, the FCC limits are more restrictive, thus taken as reference in this study.

Above 6 GHz, the IPD is a more practical quantity to be assessed, as above explained. Several definitions of *IPD* have been provided in the literature [15], however only two of them have been correlated to temperature increase [10]:

$$\mathrm{PD_n}=\frac{1}{2A}\iint_{A}\mathrm{Re}\left[\dot{E}\times\dot{H}^{*}\right]\cdot d\mathbf{A} \tag{2}$$

$$\mathrm{PD_{tot}}=\frac{1}{2A}\iint_{A}\left\|\mathrm{Re}\left[\dot{E}\times\dot{H}^{*}\right]\right\|\cdot d\mathbf{A} \tag{3}$$

where $\dot{E}$ and $\dot{H}$ are the complex peak phasor fields, $*$ is the complex conjugate operator, A is the averaging area for *IPD* calculation, $d\mathbf{A}$ is a differential vector normal to the surface. Both IPD definitions must be averaged over a squared area of 4 cm2 projected to the body surface.

III. MODELS AND METHODS

In this section, the exposure scenarios as well as simulation and experimental assessment methods are presented.

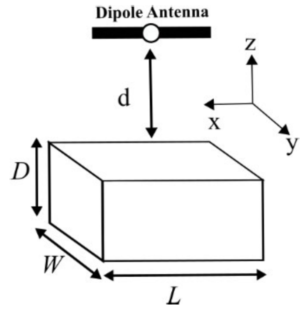

FIGURE 1. Body phantom-antenna exposure scenario.

A. EXPOSURE SCENARIOS

A flat body phantom with dimensions $L \times W \times D = 225 \times 150 \times 50$ mm^3 placed at variable distances d from the antenna is adopted as exposure scenario, as shown in Fig. 1. The body phantom is made of a tissue-equivalent liquid material at 6 GHz, i.e., with relative permittivity $\varepsilon_r' = 35.1$ and electric conductivity $\sigma = 5.48$ S/m according to [25]. The power levels were assessed at distances of $d = 2$, 5, 10, and 20 mm between the antenna and the phantom plane.

Note that in this study, the output power reference is considered at the antenna input, i.e., any detuning or distortion of the reflection coefficient due to body presence is already reflected in the SAR values and considered as part of discontinuities in final power levels.

B. NUMERICAL ASSESSMENT

Numerical simulations were performed using the commercial software Ansys®HFSS, Release 2018.1. A canonical half-wave dipole antenna made of perfect electric conductor (PEC) and designed for 6 GHz (antenna length: 24.98 mm) has been considered, as shown in Fig. 1. All simulations were truncated with perfectly matched layers (PML) boundary conditions. An adaptive meshing refinement with maximum element length no greater than 5 mm and additional restrictions over all power density calculation planes was applied. The electromagnetic field data was finally exported along a rectilinear grid with 1 mm resolution in order to determine compliance with SAR and IPD limits.

The SAR values were averaged over a 1 g mass and the maximum allowed power levels were determined when the SAR_{1g} value reached the FCC limit of 1.6 W/kg. Meanwhile, the maximum allowed powers were also determined using the FCC IPD limit of 10 W/m^{2}averaged over a square-shaped area of 4 cm^2. Both IPD definitions expressed by Eqs. (2) and (3) were evaluated.

C. MEASURMENT ASSESSMENT

Both SAR and PD measurements were performed with the Speag Dasy 6 system. SAR measurements were performed using an isotropic E-field probe in a body phantom [26]. The PD measurements were performed using a mmWave probe (750 MHz - 110 GHz) in free space. In this case, the E-field was measured, and the H-field was reconstructed to obtain PD values [27]. Two types of algorithms are generally used for the H-field reconstruction: the Plane-to-Plane (PP) method and the Equivalent Source Reconstruction (ESR) [28].

The check of dielectric parameters is done prior to the use of the tissue simulating liquid. The verification is made by comparing the relative permittivity and conductivity to the values recommended by the applicable standards [25].

The expanded uncertainty of SAR measurement system is around 23% and for incident power density is around 2.68 dB.

TABLE 2. Dipole antenna simulation: maximum incident power (dBm) to be compliant with FCC SAR limit (1.6 W/kg) and IPD limit (10 W/m^2).

d (mm)	SAR 1g mass avg.	PD_n 4 cm^2 area avg.	PD_{tot} 4 cm^2 area avg.
2	5.27	10.05	7.71
5	8.96	11.28	10.11
10	15.51	13.29	11.58
20	21.55	16.70	16.47

TABLE 3. Dipole antenna measurement: maximum incident power (dBm) to be compliant with FCC SAR limit (1.6 W/kg) and IPD limit (10 W/m^2).

d (mm)	SAR 1 g mass avg.	PD_n 4 cm^2 area avg.	PD_{tot} 4 cm^2 area avg.
2	8.25	12.21	11.25
5	11.91	13.78	13.43
10	16.14	16.04	15.72
20	20.58	19.66	19.20

IV. NUMERICAL RESULTS

Table 2 shows the simulated results for the half-wave dipole antenna at 6 GHz. It lists the maximum allowed incident power to be compliant with the FCC SAR and IPD limits, respectively, for different distances from 2 mm to 20 mm. The table is showing that at various distances, SAR AND IPD limits allow different maximum antenna incident power. At close distances, E.g., 2 mm AND 5 MM, SAR is more restrictive leading TO lower power transmission compared TO THE ipd restriction. However, at further distances, E.g., 10 mm and 20 mm, IPD becomes more restrictive and defines THE incident power level

V. MEASUREMENT RESULTS

Measurements results for the Dipole and PIFA antennas are reported in Tables 3 and 4, respectively. As can be observed a higher power can be allowed for the PIFA compared to the dipole antenna, given the PIFA is less directional.

Fig. 2 shows the comparison between simulations and measurements for SAR and IPD for the dipole antenna. This figure shows the same trends and behavior for maximum power variation vs. distances between simulation and measurement

TABLE 4. PIFA antenna measurement: maximum incident power (dBm) to be compliant with FCC SAR limit (1.6 W/kg) and IPD limit (10 W/m^2).

d (mm)	SAR 1g mass avg.	PD_n 4 cm^2 area avg.	PD_{tot} 4 cm^2 area avg.
2	16.45	18.48	17.62
5	19.84	21.04	20.35
10	26.02	25.11	24.82
20	31.25	27.91	27.17

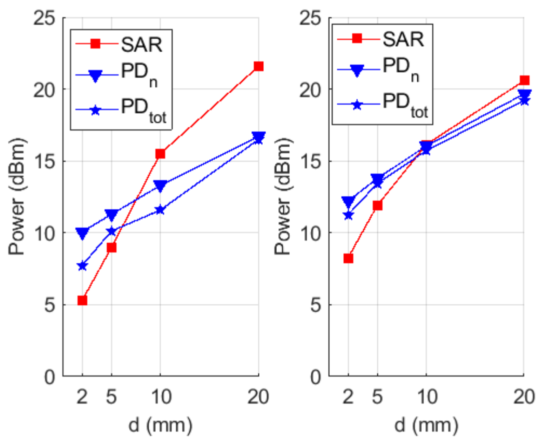

FIGURE 2. Simulated (left) and measurement (right) of SAR (1 g mass avg.) and IPD (4 cm^2 area avg.) limited output power level (dBm) for the dipole antenna at 6 GHz.

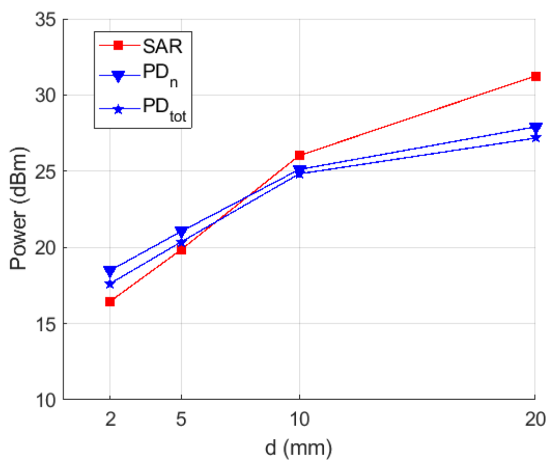

FIGURE 3. Measurement of SAR (1 g mass avg.) and IPD (4 cm^2 area avg.) limited output power level (dBm) for PIFA antenna at 6 GHz.

for all metrics. The difference in absolute values may be related to the variability of body model, and to the difference between the canonical dipole antenna simulated model and the manufactured model used in measurement as well as numerical errors of simulations, specially in the reactive near-field [10].

Fig. 3 shows the measurement results for SAR and IPD using the PIFA. Both Figs. 2 and 3 show that the SAR metric is more conservative (transmitted power is limited) at close distances, e.g., 2 mm. There is a flip between 5 and 10 mm, where the IPD defines the incident power level.

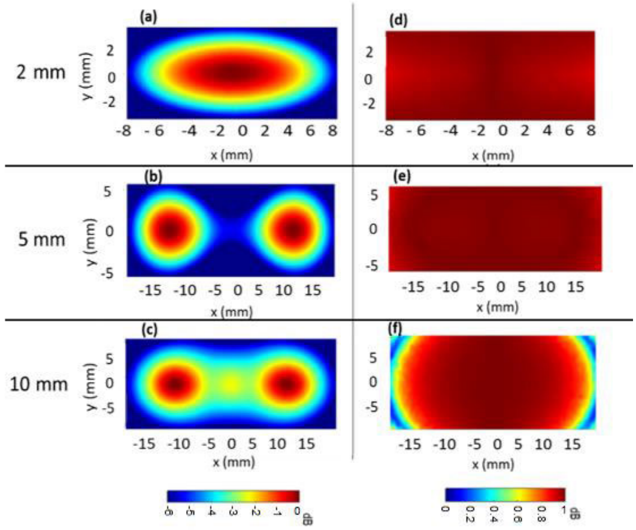

FIGURE 4. Normalized E-field (log scale) for dipole at (a) 2 mm (b) 5 mm and (c) 10 mm. Ratios of E-field tangential component to the total magnitude (linear scale) for dipole at (d) 2 mm (e) 5 mm and (f) 10 mm.

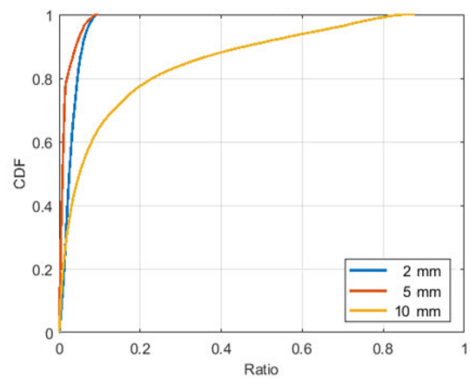

FIGURE 5. CDF of the E-field normal component to magnitude ratios.

In order to explain this behavior, the dipole antenna was considered. The normalized E-field distributions at 2, 5 and 10 mm separation distances in the zone of the 6 dB maximum to minimum ratio are presented in Fig. 4(a-c). The distance of 20 mm is not considered because the flip between the two metrics is already occurred. The corresponding distributions of ratios between the E-field tangential component to the magnitude at the boundaries between the free space and body model are showed in Fig. 4(d-f).

These figures show that going from 2 mm to 10 mm the contribution of E-field tangential component tends to decrease. This means that for further distances (within the near field) the E-field has more contributors related to normal components. According to the EMF boundaries conditions, the normal component is attenuated by the presence of body, which is not the case for tangential components. This may explain why at a specific distance the PD metric (in free space) becomes more conservative compared to the SAR metric (in body liquid).

The level of contributions of the normal component at each distance planes presented in Fig. 4 is illustrated in Fig. 5 using the Cumulative Distribution Function (CDF) of the normal component to magnitude ratios. This figure shows that the normal component ratio at 10 mm is higher compared to 2 and 5 mm confirming the previous assumptions.

VI. DISCUSSION AND CONCLUSION

International safety standards/guidelines have recently revised the exposure limits around 6 GHz, where the dosimetric exposure metric changes from the specific absorption rate (SAR) to the epithelial/absorbed power density (E/A-PD). Since the latter is still difficult to be measured, despite it is the recommended metric in the reactive near-field, the incident power density (IPD) is practically used as compliance metric above 6 GHz creating a discontinuity with SAR limits (below 6 GHz) in the maximum allowable output power.

This paper therefore studies the power level discontinuity produced by those RF sources, such as 5G and Wi-Fi®6E, working around the transition frequency of 6 GHz. The study was performed at several exposure distances using either a dipole antenna and a Planar Inverted F Antenna (PIFA) by means of numerical simulations as well as experimental measurements. The assessment was based on the comparison between the maximum allowable power values obtained while remaining compliant to the SAR and IPD limits for the same exposure conditions. From this assessment, two key points can be drawn:

1) At the 6 GHz transition frequency, the SAR metric is more conservative at very close distances i.e., below $0.15\,\lambda$, then the conservativeness is flipped, and the IPD becomes more conservative above $0.15\,\lambda$.
2) At a specific distance, there is a discontinuity in terms of maximum allowed power related to EMF exposure limits. This difference tends to become larger (up to 6 dB) at very close distances ($\leq 0.1\lambda$) and relatively far distances ($> 0.2\lambda$).

With the growing interest for new wireless technologies utilizing frequency bands around 6 GHz, it is important that the inconsistencies at the transition frequency from SAR to PD based limits are timely solved. If not, the observed discrepancy might have a large impact on the development of future mobile communication networks. Therefore, it is strongly encouraged that relevant standardization bodies and regulatory authorities responsible for defining EMF exposure limits will address this issue in the next future.

REFERENCES

[1] E. Dahlman, S. Parkvall, and J. Skold, *5G NR: The Next Generation Wireless Access Technology*. New York, NY, USA: Academic, 2018.

[2] A. Osseiran, S. Parkvall, P. Persson, A. Zaidi, S. Magnusson, and K. Balachandran, "5G wireless access: An overview," Ericsson, Stockholm, Sweden, White Paper 1/28423-FGB1010937, Apr. 2020.

[3] *Wi-Fi Alliance, Wi-Fi CERTIFIED 6*. Accessed: Dec. 15, 2022. [Online]. Available: https://www.wi-fi.org/discover-wi-fi/wi-fi-certified-6

[4] *IEEE Standard for Safety Levels With Respect to Human Exposure to Electric, Magnetic and Electromagnetic Fields*, Standard IEEE-C95.1, 0 Hz to 300 GHz, 2019.

[5] International Commission on Non-Ionizing Radiation Protection, "Guidelines for limiting exposure to electromagnetic fields (100 kHz to 300 GHz)," *Health Phys.*, vol. 118, no. 5, pp. 483–524, May 2020.

[6] V. Anderson, R. Croft, and R. L. McIntosh, "SAR versus S_{inc}: What is the appropriate RF exposure metric in the range 1–10 GHz? Part I: Using planar body models," *Bioelectromagnetics*, vol. 31, pp. 454–466, Sep. 2010.

[7] R. L. McIntosh and V. Anderson, "SAR versus S_{inc}: What is the appropriate RF exposure metric in the range 1–10 GHz? Part II: Using complex human body models," *Bioelectromagnetics*, vol. 31, pp. 467–478, Sep. 2010.

[8] D. Colombi, B. Thors, and C. Törnevik, "Implications of EMF exposure limits on output power levels for 5G devices above 6 GHz," *IEEE Antennas Wireless Propag. Lett.*, vol. 14, pp. 1247–1249, 2015.

[9] K. Li, S. Kodera, D. Poljak, Y. Diao, K. Sasaki, A. Susnjara, A. Prokop, K. Taguchi, J. Xi, S. Zhang, M. Yao, G. Sacco, M. Zhadobov, W. E. Hajj, and A. Hirata, "Calculated epithelial/absorbed power density for exposure from antennas at 10–90 GHz: Intercomparison study using a planar skin model," *IEEE Access*, vol. 11, pp. 7420–7435, 2023.

[10] V. De Santis, A. D. Francesco, G. Bit-Babik, J. Roman, and W. E. Hajj, "On the correlation between incident power density and temperature increase for exposures at frequencies above 6 GHz," *IEEE Access*, vol. 10, pp. 82236–82245, 2022.

[11] K. Li, Y. Diao, K. Sasaki, A. Prokop, D. Poljak, V. Doric, J. Xi, S. Kodera, A. Hirata, and W. E. Hajj, "Intercomparison of calculated incident power density and temperature rise for exposure from different antennas at 10–90 GHz," *IEEE Access*, vol. 9, pp. 151654–151666, 2021.

[12] S. Omi, K. Sasaki, and K. Wake, "Performance analysis of incident power density evaluation by inverse source method for compliance assessment at quasi-millimeter and millimeter wave bands," *IEEE Trans. Electromagn. Compat.*, vol. 63, no. 5, pp. 1649–1657, Oct. 2021.

[13] Y. Diao, E. A. Rashed, and A. Hirata, "Assessment of absorbed power density and temperature rise for nonplanar body model under electromagnetic exposure above 6 GHz," *Phys. Med. Biol.*, vol. 65, no. 22, Nov. 2020, Art. no. 224001.

[14] W. He, B. Xu, Y. Yao, D. Colombi, Z. Ying, and S. He, "Implications of incident power density limits on power and EIRP levels of 5G millimeter-wave user equipment," *IEEE Access*, vol. 8, pp. 148214–148225, 2020.

[15] T. Nakae, D. Funahashi, J. Higashiyama, T. Onishi, and A. Hirata, "Skin temperature elevation for incident power densities from dipole arrays at 28 Ghz," *IEEE Access*, vol. 8, pp. 26863–26871, 2020.

[16] A. Christ, T. Samaras, E. Neufeld, and N. Kuster, "Limitations of incident power density as a proxy for induced electromagnetic fields," *Bioelectromagnetics*, vol. 41, no. 5, pp. 348–359, May 2020.

[17] K. Sasaki, K. Li, J. Chakarothai, T. Iyama, T. Onishi, and S. Watanabe, "Error analysis of a near-field reconstruction technique based on plane wave spectrum expansion for power density assessment above 6 GHz," *IEEE Access*, vol. 7, pp. 11591–11598, 2019.

[18] A. Hirata, D. Funahashi, and S. Kodera, "Setting exposure guidelines and product safety standards for radio-frequency exposure at frequencies above 6 GHz: Brief review," *Ann. Telecommun.*, vol. 74, nos. 1–2, pp. 17–24, Feb. 2019.

[19] K. Li, K. Sasaki, S. Watanabe, and H. Shirai, "Relationship between power density and surface temperature elevation for human skin exposure to electromagnetic waves with oblique incidence angle from 6 GHz to 1 THz," *Phys. Med. Biol.*, vol. 64, no. 6, Mar. 2019, Art. no. 065016.

[20] T. Samaras and N. Kuster, "Theoretical evaluation of the power transmitted to the body as a function of angle of incidence and polarization at frequencies >6 GHz and its relevance for standardization," *Bioelectromagnetics*, vol. 40, no. 2, pp. 136–139, Feb. 2019.

[21] *Code of Federal Regulations CFR Title 47, Part 1.1310*, FCC, Federal Commun. Commission, Washington, DC, USA, 2020.

[22] *Assessment of Power Density of Human Exposure to Radio Frequency Fields From Wireless Devices in Close Proximity to the Head and Body (Frequency Range of 6 GHz to 300 GHz)—Part I: Measurement Procedure*, Standard IEC/IEEE FDIS 63195-1, 2021.

[23] *Assessment of Power Density of Human Exposure to Radio Frequency Fields From Wireless Devices in Close Proximity to the Head and Body (Frequency Range of 6 GHz to 300 GHz)—Part II: Computational Procedure*, Standard IEC/IEEE FDIS 63195-2, 2022.

[24] *Conversion Method of Specific Absorption Rate to Absorbed Power Density for the Assessment of Human Exposure to Radio Frequency Electromagnetic Fields From Wireless Devices in Close Proximity to the Head and Body—Frequency Range of 6 GHz to 10 GHz*, Standard IEC PAS 63446, 2022.

[25] *Measurement Procedure for the Assessment of Specific Absorption Rate of Human Exposure to Radio Frequency Fields From Hand-Held and Body-Worn Wireless Communication Devices—Human Models, Instrumentation, and Procedures (Frequency Range of 4 MHz to 10 GHz)*, Standard IEC/IEEE 62209-1528, 2020.

[26] *DASY8 Module SAR Manual*, Schmid & Partner Engineering AG, Zürich, Switzerland, Apr. 2022.

[27] *DASY8 Module mmWave Manual*, Schmid & Partner Engineering AG, Zürich, Switzerland, Feb. 2022.

[28] *DASY8 Application Note: SAR, APD & PD at 6–10 GHz (Version 5)*, Schmid & Partner Engineering AG, Zürich, Switzerland, Apr. 2022.

WALID EL HAJJ (Member, IEEE) received the National Degree of Master for his research in microwave materials and devices for communication systems and the Ph.D. degree in information and communications sciences and technologies from Telecom Bretagne, Brest, France, in 2008 and 2011, respectively.

From 2011 to 2013, he was a Researcher with the Department of Microwave, Lab-STICC/MOM Laboratory, Telecom Bretagne. He joined Intel Corporation, in 2014. He is currently a Scientist Officer with the Wireless Test and Certification Center Group. He is also leading the different research and development activities related to new wireless technologies and products certification. He is participating and leading several standardization efforts in the human exposure and product safety domain. He is mandated as an Expert of the French Standardization Association (AFNOR). Since 2017, he has been participating in the development of several IEEE/IEC standards on human exposure computational and measurement assessments. He is also the Co-Convener of IEC/IEEE JWG12 developing measurement methods standards to assess the power density in close proximity to the head and body from 6–300 GHz.

Dr. El Hajj is a member of IEC TC 106 and IEEE ICES TC95. He is also a member of CMC TF Radio Group in IECEE. He was the Chair of WG 5 under SC 6 of IEEE ICES TC95 that published the guide IEEE 2889-2021 studying the different aspects of incident power density definition publishing.

JOHN ROMAN (Senior Member, IEEE) was born in Dallas, TX, USA, in 1961. He received the B.S. degree in electrical engineering and the M.S. degree in electrical engineering from Florida Atlantic University (FAU), Boca Raton, FL, USA, in 1988 and 1998, respectively, with a focus on antenna theory. He was a Research Faculty Member at FAU, from 1990 to 1995, as the Associate Director of the EMI Research and Development Laboratory, the Compliance Manager of ECI Telecom, from 1995 to 2000, and joined Intel Corporation, Hillsboro, OR, USA, in 2000, where he is currently the Director of Broadband and Regulatory Policy. He is also a member of the 5G Automotive Association, where he is the Vice Chair of the Regulatory Working Group. He is currently the Co-Convenor of IEC/IEEE 63195-2 ED1, Assessment of Power Density of Human Exposure to Radio Frequency Fields from Wireless Devices in Close Proximity to the Head and Body (Frequency Range from 6 GHz to 300 GHz)—Part 2: Computational Procedure. He has published several papers in IEEE journals and conference proceedings, for example most recently such as Teruo Onishi; Kai Niskala; Andreas Christ; John Roman, Exposure assessment methods with respect to the 5G mobile communication systems, and 2020 International Symposium on Electromagnetic Compatibility—EMC EUROPE, in September 2020.

ZHEN YAO (Member, IEEE) received the B.S. degree in physics from Nankai University, Tianjin, China, in 2004, and the Ph.D. degree in applied physics from Case Western Reserve University, Cleveland, OH, USA. In 2014, he joined Intel Corporation as an RF Engineer involved in wireless charging technology and EMI/RFI mitigation. He is currently a Quality Reliability Engineer involved in chip reliability modeling. He has coauthored more than ten research journal articles and 20 U.S. patents covering MRI coil designs, wireless charging technology, and RF exposures, and a book chapter on wireless power transfer by magnetic induction. He is currently a member of IEEE ICES TC95.

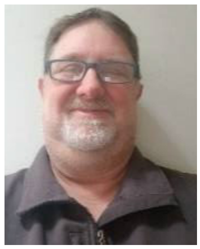

ROBERT PAXMAN (Member, IEEE) received the A.A.S. degree from ITT, in 1994. He started his journey as a Regulatory Engineer with Compatible Electronics as a Telecommunications Test Engineer and after serving six years in the U.S. Army as a 52D Generator Mechanic. He move to wireless regulations occurred with Xircom, from 1999 to 2001, where he obtained the industry's first 5 GHz Wi-Fi portable FCC certification. He is currently a Wireless Regulatory Engineer with Intel Corporation, where he has been employed for 22 years. More than 25 years of experience as a Regulatory Engineer, he has not only contributed to standard development within ANSI but has also been a key contributor in regulatory advocacy globally both directly with government entities and in collaboration with ITI, MWF, and other trade associations. He has also collaborated and contributed on five patent filings in which three have been granted thus far. Most recently, he was nominated for a 2-year term on the Board of Directors with the TCBC. He has served as the TG Chair within ANSI C63.10 and C63.26 for mmWave and vehicular radar test measurements. He is also the ITIC TC8 Chair.

VALERIO DE SANTIS (Senior Member, IEEE) received the Laurea degree (Hons.) in telecommunication engineering and the Ph.D. degree in electrical and computer engineering from the University of L'Aquila, L'Aquila, Italy, in 2006 and 2010, respectively. He joined the Foundation for Research on Information Technologies in Society (IT'IS), Switzerland, from 2011 to 2013, holding the position of the Project Leader. He was an Assistant Professor with the Nagoya Institute of Technology, Nagoya, Japan, from January 2015 to March 2015. He is currently an Associate Professor with the University of L'Aquila. His current research interests include wireless power transfer, numerical methods and techniques, electromagnetic compatibility, and human exposure safety. He is participating in and leading several standardization efforts in the human exposure and product safety domain. He is a member of IEC TC 106 and IEEE ICES TC95. He was a recipient of the Second Best Student Paper Award from the Bioelectromagnetics Society (BEMS) Annual Meeting, Cancun, Mexico, in 2006; the Best Student Paper Award from the IEEE International Symposium on EMC, Honolulu, USA, in 2007; and the Leo L. Beranek Travel Grant from the IEEE International Symposium on EMC, Detroit, USA, in 2008.

Open Access funding provided by 'Università degli Studi dell'Aquila' within the CRUI CARE Agreement